

Excitation transfer among, and quenching of, the barium $6s5d\ ^3D_J$ metastable levels due to collisions with argon, nitrogen, and barium perturbers

E. Ehrlicher and J. Huennekens

Department of Physics, Lehigh University, 16 Memorial Drive East, Bethlehem, Pennsylvania 18015

(Received 29 November 1993)

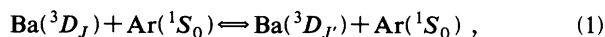
We describe a set of experiments that investigate excitation transfer among the barium $6s5d\ ^3D_J$ metastable levels due to collisions with argon perturber atoms, and quenching of atoms in these levels by nitrogen perturber molecules. The metastable levels were populated through optical pumping of the $6s^2\ ^1S_0 \rightarrow 6s6p\ ^3P_1^o$ intercombination transition with a pulsed laser, followed by stimulated emission or stimulated Raman scattering into the $6s5d\ ^3D_{1,2}$ levels. Collisional mixing then distributed population throughout the 3D_J levels. Time-dependent absorption coefficients were obtained by measuring the transmission of a weak cw probe laser beam (after the pulsed laser fired) at several perturber number densities. Argon buffer gas was used to investigate fine-structure mixing, and nitrogen was used to study quenching. The time-dependent absorption coefficients were fitted to appropriate fitting functions, obtained by solving the set of coupled rate equations used to model the time evolution of the metastable level populations. The buildup rates of the initially unpopulated 3D_3 and underpopulated 3D_1 levels were used to determine the collisional mixing rates, while the measured decay rates of the 3D_J level populations yielded the quenching rates. From plots of buildup rates versus argon number density for the $^3D_{1,3}$ states, we were able to determine four of the six fine-structure mixing rate coefficients k_{ij} . The results are $k_{12} = (1.71 \pm 0.18)$, $k_{21} = (1.39 \pm 0.13)$, $k_{23} = (1.42 \pm 0.13)$, and $k_{32} = (1.92 \pm 0.16) \times 10^{-13}\ \text{cm}^3\ \text{s}^{-1}$. The experiment is not sensitive to the values of k_{13} and k_{31} . Estimated rate coefficients for excitation transfer among the 3D_J levels due to collisions with barium atoms are $k_{21}^{\text{Ba}} = 1.3 \times 10^{-10}\ \text{cm}^3\ \text{s}^{-1}$ and $k_{23}^{\text{Ba}} = 5.8 \times 10^{-10}\ \text{cm}^3\ \text{s}^{-1}$. A plot of the population decay rates versus N_2 number density for each of the three metastable levels yielded the average nitrogen quenching rate coefficient $k_q = (3.14 \pm 0.19) \times 10^{-11}\ \text{cm}^3\ \text{s}^{-1}$.

PACS number(s): 32.50.+d

I. INTRODUCTION

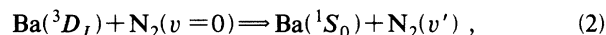
The lowest excited energy states of barium are the $6s5d\ ^3D_J$ levels which are metastable due to the absence of dipole allowed radiative transitions (see Fig. 1). Because of their long lifetimes, these levels are of interest as an energy storage medium and for use in narrow-band atomic line filters [1]. Recently, we have also begun a study of the effects of these metastable levels on the non-linear optical response of barium. In our efforts to characterize these states, we have carried out studies of the broadening, due to collisions with argon and helium perturbers, of various transitions whose lower levels are one of the metastable 3D_J states [2]. The results of these studies have given us an accurate means of determining populations in each of the 3D_J fine-structure levels over a wide range of conditions.

In the present report, we describe a series of time-resolved measurements which were carried out to study the population and depopulation mechanisms of these metastable levels. In particular, we present measured rate coefficients for excitation transfer among the metastable fine-structure levels (fine-structure mixing) due to collisions with argon atoms,



and for quenching of the metastables by collisions with

diatomic nitrogen molecules,



where $\text{N}_2(v')$ represents a vibrationally excited nitrogen molecule. We are also able to estimate the rate of fine-structure mixing, and put an upper limit on the rate for quenching, due to collisions with ground-state barium atoms. Section II of this paper presents a rate equation model which shows how time-dependent populations are related to the various rate coefficients of interest. Section III then presents a brief description of the experiment, and Sec. IV presents the results. A brief discussion of the results and our conclusions are given in Sec. V.

II. THEORY

Collisional mixing and quenching of barium atoms in the metastable 3D_J levels are modeled using the standard technique of solving coupled rate equations for the populations. In our experiments, we use a short pulse laser to excite the $6s6p\ ^3P_1^o$ state (see Fig. 1). The $^3D_{1,2}$ levels are then populated rapidly by stimulated emission (due to the population inversion created between the $^3P_1^o$ and $^3D_{1,2}$ levels) and by stimulated Raman scattering of the laser light. Since this population mechanism is very rapid (occurring within the 6-ns duration of the laser pulse), we consider the metastable levels to be an isolated three-level

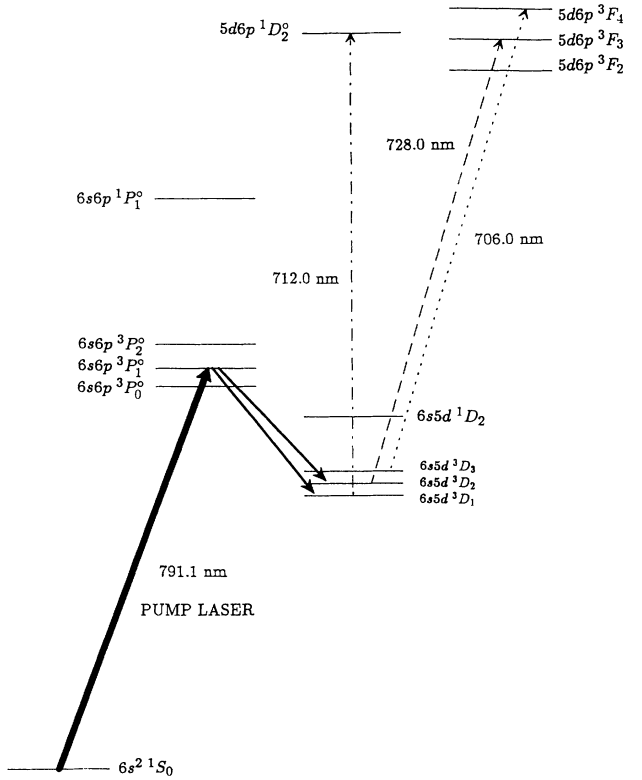


FIG. 1. Atomic energy-level diagram showing the levels of barium used in this work. The heavy solid arrow represents the pump laser, while the thin solid arrows represent the stimulated emission channels which populate the $6s5d^3D_{1,2}$ levels. The dashed lines denote the three probe laser transitions used in these experiments. Note that the level splittings for the $6s6p^3P_{0,1,2}$ and $6s5d^3D_{1,2,3}$ multiplets are exaggerated for clarity.

system with the following initial conditions for the level number densities:

$$n_1(0) = N_1, \quad n_2(0) = N_2, \quad n_3(0) = 0. \quad (3)$$

Here the subscripts 1, 2, and 3 refer to the $^3D_{1,2,3}$ states, respectively. Using these initial conditions, we can neglect processes involving the ground (1S_0) and $^3P_1^o$ states and write the following coupled rate equations to describe the time evolution of the metastable state number densities:

$$\dot{n}_3 = R_{13}n_1 + R_{23}n_2 - (R_{31} + R_{32} + Q_3)n_3, \quad (4a)$$

$$\dot{n}_2 = R_{12}n_1 - (R_{21} + R_{23} + Q_2)n_2 + R_{32}n_3, \quad (4b)$$

$$\dot{n}_1 = -(R_{12} + R_{13} + Q_1)n_1 + R_{21}n_2 + R_{31}n_3. \quad (4c)$$

Here Q_i is the quenching rate out of level i , and R_{ij} is the excitation transfer term (collisional mixing rate) from level i to level j . Although Eqs. (4) contain three quenching rates and six mixing rates, the latter can be reduced to three by applying the principle of detailed balance:

$$\frac{R_{ij}}{R_{ji}} = \frac{g_j}{g_i} e^{-(E_j - E_i)/kT} \equiv \alpha_{ij}, \quad (5)$$

where $g_j = 2j + 1$ is the degeneracy and E_j is the energy of level j . The mixing and quenching rate coefficients k_{ij} and k_q^i are related to the mixing and quenching rates by

$$R_{ij} = k_{ij}n_p \quad (6)$$

and

$$Q_i = k_q^i n_p, \quad (7)$$

where n_p is the perturber atom or molecule density.

The general solution to Eqs. (4) is a triple exponential decay for each of the three coupled levels. The exponential decay constants are related to the mixing and quenching rates. However, the relationships are complicated, and it is useful to make further simplifications in order to apply this model in the limits we wish to examine.

A. Excitation transfer among the 3D_J sublevels through collisions with argon perturbers

Experimentally we find that argon is very ineffective at quenching barium atoms in the $6s5d^3D_J$ sublevels. Over a time period of at least several hundred microseconds, no evidence of quenching of these atoms by argon has been observed. In fact, the quenching by argon is so slow that the dominant decay mechanism for the metastable atoms in an argon buffer gas is diffusion of the metastables out of the excitation region.

In this situation, quenching can be neglected in Eqs. (4), and the general solution to the coupled rate equations can be written as

$$n_i(t) = A_i + B_i e^{-\omega_- t} + C_i e^{-\omega_+ t}. \quad (8)$$

Coupled rate equations of the form of Eqs. (4) (with all the Q_i 's equal to zero) for the $4s4p^3P_J$ levels of calcium have been solved by Beitia *et al.* [3] with the initial conditions $n_1(0) = n_2(0) = 0$ and $n_3(0) = N_0$. The complete solution from this reference [which can also be obtained directly by solving Eqs. (4)] is too long to be reproduced here. However, the exponential buildup and decay rates are given by

$$\omega_{\pm} = \frac{1}{2}(e + b) \pm \frac{1}{2}\sqrt{(e - b)^2 + 4ad}, \quad (9)$$

with

$$\begin{aligned} a &= R_{21} - R_{31}, \quad b = R_{12} + R_{13} + R_{31}, \quad d = R_{12} - R_{32}, \\ e &= R_{21} + R_{23} + R_{32}. \end{aligned} \quad (10)$$

The slightly more complicated initial conditions used in the present work do not change the decay rates given by Eq. (9). However, the amplitudes A_i , B_i , and C_i are much more complicated than those given in Ref. [3]. Since the amplitudes are not used in our analysis to derive information about the mixing rates, they are not presented here.

B. Quenching of barium $6s5d^3D_J$ metastable atoms by N_2 perturbers

To determine the quenching rates of the metastable barium atoms by N_2 perturbers, we make the assumption

of complete fine-structure mixing; i.e., we assume that the $6s5d^3D_J$ levels are populated in a ratio given by their statistical weights multiplied by a Boltzmann factor. This assumption is reasonable since our data show that the buildup of population in the initially unpopulated 3D_3 state is fast compared to the decay (quenching) rates for all N_2 pressures. Under this assumption, all the R_{ij} terms in Eqs. (4) cancel, and we are left with three equations of the form

$$\dot{n}_i = -Q_i n_i, \quad (11)$$

which has the solution

$$n_i(t) = n_i(0)e^{-Q_i t}. \quad (12)$$

This result presents us with the misleading idea that we can measure an independent quenching rate for each 3D_J level. However, as the system evolves, the populations remain in statistical equilibrium due to fine-structure mixing:

$$\begin{aligned} n_i &= \frac{g_i e^{-E_i/kT}}{g_1 e^{-E_1/kT} + g_2 e^{-E_2/kT} + g_3 e^{-E_3/kT}} n \\ &= \frac{1}{\alpha_{i1} + \alpha_{i2} + \alpha_{i3}} n \equiv \gamma_i n. \end{aligned} \quad (13)$$

Thus if one level is quenched faster than the others, collisional mixing would quickly restore statistical equilibrium. In this limit, the best we can hope to achieve is to measure a statistically weighted average of the individual level quenching rates. Under these conditions, it can be shown that all three metastable level populations decay with the same rate

$$\begin{aligned} \omega_- = Q_{\text{eff}} &= \gamma_1 Q_1 + \gamma_2 Q_2 + \gamma_3 Q_3 \\ &= 0.316Q_1 + 0.391Q_2 + 0.293Q_3, \end{aligned} \quad (14)$$

where in the last step we have evaluated the γ_i 's for the typical oven temperature of 875 K that was used in the quenching measurements.

III. THE EXPERIMENT

Barium metal is contained in a five-arm cross heat-pipe oven [4] (see Fig. 2). During the experiment, the oven was filled with a variable amount of either argon (prepurified grade) or nitrogen gas. The gas was continuously admitted to the oven and slowly pumped so that its pressure could be monitored continuously, and so that impurities baking off the oven walls would not accumulate. Gas pressures were measured with a thermocouple gauge and a capacitance manometer with ranges of 0–2000 mTorr and 0–100 Torr, respectively. (A Wallace-Tiernan gauge with range 0–800 Torr was also available.) Typical operating pressure ranges were 2–50 Torr for argon and 0.5–10 Torr for nitrogen. The oven was heated using resistance heaters to a temperature of 857 K in the mixing experiments, and 875 K for the quenching measurements. Thus the barium vapor density was approximately 1 mTorr, and the oven was clearly

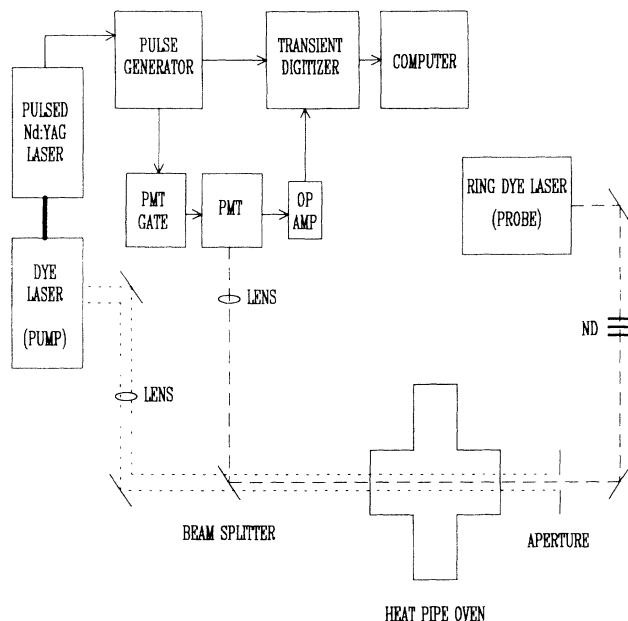


FIG. 2. Experimental setup used for both the quenching and mixing experiments. The probe and pump laser beam paths are represented by long and short dashed lines, respectively. Arrows denote electrical connections. PMT and ND denote photomultiplier tube and neutral density filters, respectively.

not operating in the "heat-pipe mode."

Barium was pumped into the metastable 3D_J levels in the following manner. A pulsed Nd:YAG (yttrium aluminum garnet) laser-pumped dye laser was tuned to the $6s^2^1S_0 \rightarrow 6s6p^3P_1^o$ intercombination line at 791.13 nm. Stimulated processes then populated the 3D_2 and to a lesser extent the 3D_1 metastable levels. Time-dependent densities in the three 3D_J levels were then probed using a counterpropagating single-mode cw ring dye laser. The ring laser frequency was tuned into resonance with either the $6s5d^3D_1 \rightarrow 5d6p^1D_2^o$, the $6s5d^3D_2 \rightarrow 5d6p^3F_3$, or the $6s5d^3D_3 \rightarrow 5d6p^3F_4$ transition, at 712.0, 728.0, and 706.0 nm, respectively. Since we had previously measured the absorption cross sections $\sigma_v = k_v/n$ (where k_v is the absorption coefficient and n is the density of atoms in the lower level of the transition), as a function of frequency for each of these transitions, we could determine the density of atoms in a selected metastable level by monitoring the absorption coefficient k_v at any selected detuning about the appropriate transition. For quenching measurements with N_2 gas, all three transitions were monitored at line center. For fine-structure mixing experiments with argon, the $6s5d^3D_1 \rightarrow 5d6p^1D_2^o$ and $6s5d^3D_3 \rightarrow 5d6p^3F_4$ transitions were monitored, but with a detuning of approximately 2–4 GHz from line center. In this case, if the laser was tuned too close to line center, the probe laser transmission was nearly zero for all times following the pulsed laser firing. However, we have verified that data recorded using different detunings on both sides of a transition are consistent. Experimentally, the transmitted ring laser intensity was detected by a gated photomultiplier (PMT in Fig. 2), and the

signal was recorded on a transient digitizer (Tektronix model 7912 HB) which averaged data over 64 shots of the pulsed laser. The PMT gating circuit pulsed the photomultiplier on for up to 200 μsec . Digitizer traces were sent to a computer for analysis. Figure 3 shows a series of typical digitizer traces obtained in the N_2 quenching experiment. Note that the digitizer was pretriggered using a pulse generator with variable delay, so that the pulsed laser fired at approximately 4.5 μsec on these traces. From the data of Fig. 3, it is easy to construct a plot of absorption coefficient versus time using the expression $I_\nu(L) = I_\nu(0)e^{-k_\nu L}$. Here $I_\nu(0)$ and $I_\nu(L)$ are the incident and transmitted probe laser intensities at frequency ν , and L is the path length through the vapor. By normalizing the transmission data to the signal recorded before the pulsed laser fired (when the lower state of the transition under investigation was unpopulated), these data directly yield the ratio $I_\nu(L)/I_\nu(0)$. Taking the natural log of these curves then yields $-k_\nu L$. This could be further reduced using the frequency-dependent absorption cross sections to yield the density of the metastable level of interest as a function of time. However, since only relative densities are relevant to the rest of the analysis, this last step was not carried out.

In the N_2 quenching experiment, probe laser absorption traces were recorded for several N_2 gas pressures (and no argon buffer gas) up to about 10 Torr. N_2 is such an efficient quencher that pressures above 10 Torr produce decay rates which are affected by the limited time resolution of the electronics. In the argon fine-structure mixing experiments, argon pressures up to 50 Torr were used. In this case, each trace was recorded on two time scales (5 and 20 $\mu\text{sec}/\text{div}$). This was done so that we could obtain sufficient resolution of the buildup times on the shorter time scale, and observe both buildup and decay information on the longer time scale. We have verified that data recorded on different time scales are consistent.

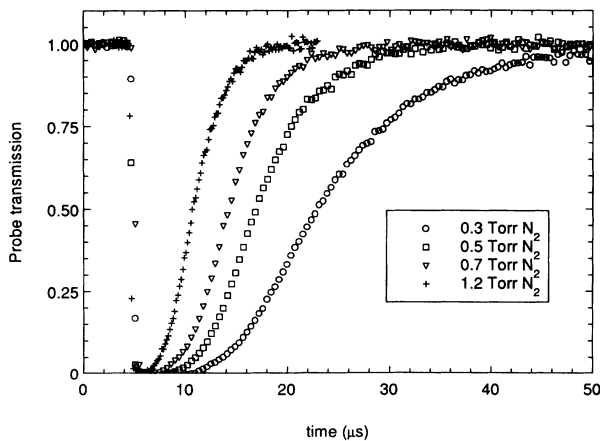


FIG. 3. Time-dependent probe beam transmission for the barium $6s5d\ ^3D_2 \rightarrow 5d6p\ ^3F_3$ transition with several N_2 buffer gas pressures and an oven temperature of 875 K. In each scan, the pump laser fires at $t = 4.5\ \mu\text{s}$.

IV. RESULTS

A. Excitation transfer among the 3D_J sublevels

According to Eq. (8), we expect to see a double exponential time dependence for the population in each metastable level in the absence of quenching. When argon is used as the buffer gas, we observe that quenching of the barium 3D_J levels is negligible. However, on the time scales with which we are interested, we must concern ourselves with diffusion of the metastable atoms out of the probe beam.

We have recently completed a study of diffusion of barium 3D_J atoms through argon [5]. There we have shown that, under the conditions of the present experiment, the number density of atoms in the 3D states at position r and time t obeys [5]

$$n_{3D}(r,t) = \frac{N_0}{\pi L} \frac{1}{r_0^2 + 4Dt} \exp\left[-\frac{r^2}{r_0^2 + 4Dt}\right]. \quad (15)$$

Here N_0 is the total number of atoms initially excited to the metastable levels, D is the diffusion coefficient, L is the length of the vapor column, and r_0 is the initial radius of the distribution of excited atoms. On axis, the metastable state density decays as $n_{3D}(r,t) \propto [r_0^2 + 4Dt]^{-1}$. Thus we can remove the effects of

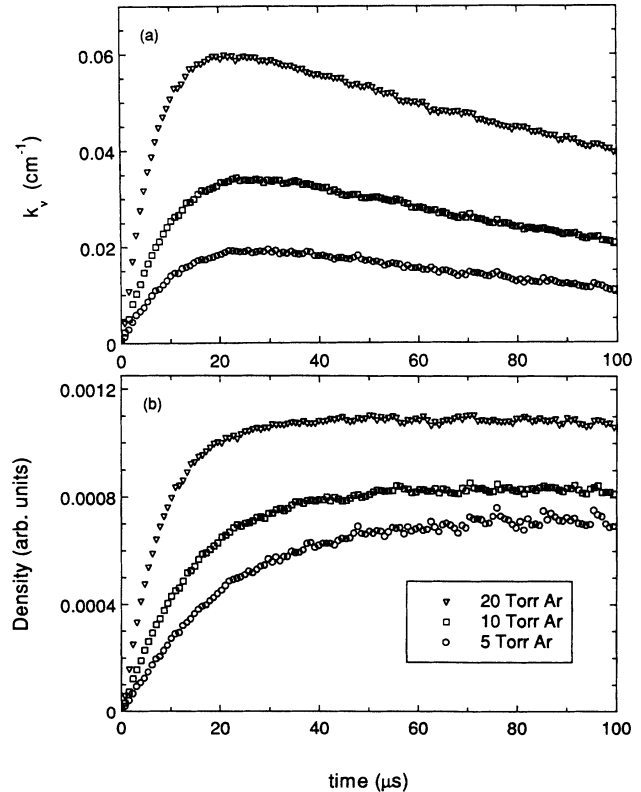


FIG. 4. (a) Time dependence of the number density in the $6s5d\ ^3D_3$ level for three different Ar buffer gas pressures. (b) The same curves after the diffusion contribution has been removed.

diffusion by multiplying our measured absorption coefficients by $[r_0^2 + 4Dt]$, using the values of r_0 and D reported in Ref. [5]. We note that the value of the diffusion cross section (from which D is determined) reported in Ref. [5] is in good agreement with the previously reported results of Ref. [6]. Figure 4(a) shows the measured buildup and decay curves (k_v versus time) for the $6s5d^3D_3$ level for three different argon pressures, while Fig. 4(b) shows the same data with the diffusion contribution removed. Note that in Fig. 4(b), the corrected number density reaches equilibrium in the late time, after complete mixing has occurred, which is as expected since there is no radiative decay from the metastable levels over this time scale.

Once the diffusion contribution is removed from the signals, they are expected to obey the double exponential form given by Eq. (8). Plots of the logarithm of the population buildup versus time should therefore show two linear regions: one with slope ω_+ and the other with slope ω_- . However, we observe a single linear dependence on these semilog plots at all buffer gas pressures, indicating that the density buildup of the metastable levels can be fit with a single exponential [7]. The population buildups (corrected for diffusion) were therefore fit by a function of the form

$$n_i(t) = n_i(\infty) + [n_i(0) - n_i(\infty)]e^{-\omega_+ t}, \quad (16)$$

where $n_i(0)$ and $n_i(\infty)$ are the initial and final number densities (or populations) in level i . All of the data could be fit well by this function. Values of ω_+ from these fits are plotted in Fig. 5, which shows the population buildup rates for the 3D_1 and 3D_3 levels (as monitored by the $6s5d^3D_1 \rightarrow 5d6p^1D_2^o$ and $6s5d^3D_3 \rightarrow 5d6p^3F_4$ transitions, respectively) as a function of argon pressure. Mixing rate coefficients k_+ for each set of data points were determined from the slopes of the least-squares straight-line fits to

$$\omega_+ = k_+ n_p. \quad (17)$$

The values $k_+ = (4.76 \pm 0.30) \times 10^{-13}$ and $(5.04 \pm 0.32) \times 10^{-13} \text{ cm}^3 \text{ s}^{-1}$ are obtained from the buildup rates for the 3D_1 and 3D_3 levels, respectively, and their weighted average yields the value

$$k_+ = (4.90 \pm 0.21) \times 10^{-13} \text{ cm}^3 \text{ s}^{-1}. \quad (18)$$

In order to determine the individual values of k_{21} and k_{23} , we need to look at the early time buildup of the populations in the $^3D_{1,3}$ levels. We can approximate the early time buildup rates by the individual mixing rates R_{21} and R_{23} since, in this limit, we can neglect back transfer because $n_2 \gg n_{1,3}$. (We have determined from our data that approximately 95% of the atoms are initially in the 3D_2 level, with the other 5% in 3D_1 .) Using this approximation, the rate equation in the very early time for the 3D_3 level density can be written as

$$\dot{n}_3 = R_{23} n_2. \quad (19)$$

Assuming that the 3D_2 level density is approximately constant [$n_2(t) \approx n_2(0) \approx n$] for times right after the

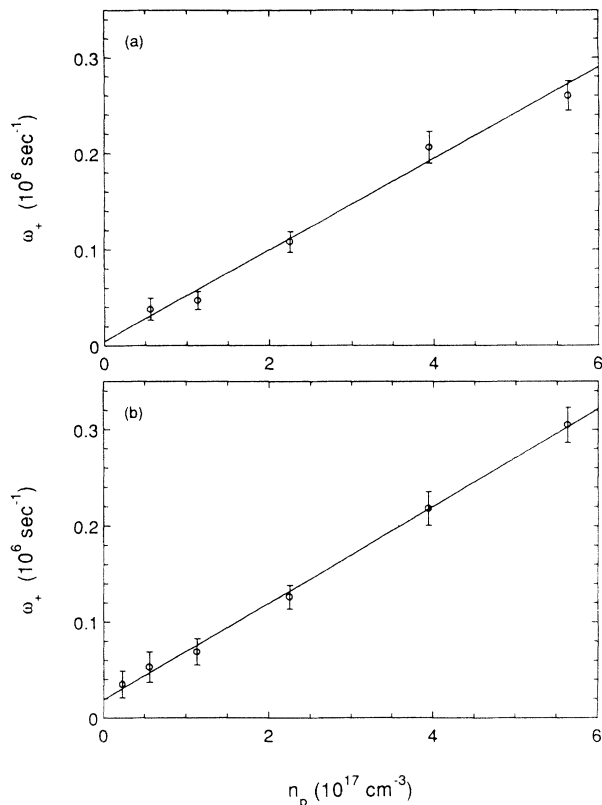


FIG. 5. Plot of the buildup rate ω_+ vs Ar number density for (a) the $6s5d^3D_1 \rightarrow 5d6p^1D_2^o$, and (b) the $6s5d^3D_3 \rightarrow 5d6p^3F_4$ transitions. The least-squares straight line fits, from which k_+ is determined, are also shown in the figure.

firing of the pulsed laser, the solution of Eq. (19) is

$$n_3(t) = n_2(0) R_{23} t. \quad (20)$$

The normalized slope of the early time data shown in Fig. 4(b) is therefore given by

$$\frac{\Delta[n_3(t)/n_3(\infty)]}{\Delta t} = \frac{n_2(0) R_{23}}{n_3(\infty)} = \frac{R_{23}}{0.289} = \omega_+, \quad (21)$$

where the ratio $n_3(\infty)/n_2(0) = n_3(\infty)/n = 0.289$ is determined from the statistical population ratios at $T = 857 \text{ K}$ [see Eq. (13)] after complete mixing has occurred. The final step of Eq. (21) was obtained by expanding the exponential solution [Eq. (16)] in the early time. Thus we find that $R_{23} = 0.289 \omega_+$ and $k_{23} = 0.289 k_+$.

k_{21} is determined from the early time build up of the 3D_1 level density in a similar manner, except in this case we need to account for the initial (small) population in the 3D_1 level [$n_1(0) = 0.05n$], and only the relevant results are summarized below. The normalized early time slope is

$$\frac{\Delta[n_1(t)/n_1(\infty)]}{\Delta t} = \left[\frac{n}{n_1(\infty)} - \frac{n_1(0)}{n_1(\infty)} \right] R_{21} = \frac{R_{21}}{0.336}. \quad (22)$$

Here $(n_1(\infty)/n) = 0.319$ and

$$(n_1(0)/n_1(\infty)) = \left[\frac{n_1(0)/n}{n_1(\infty)/n} \right] = \frac{0.05}{0.319} = 0.157$$

at $T = 857$ K. The slope determined by expanding the exponential solution [Eq. (16)] for small t is

$$\frac{\Delta[n_1(t)/n_1(\infty)]}{\Delta t} = \left[1 - \frac{n_1(0)}{n_1(\infty)} \right] \omega_+ = 0.843\omega_+. \quad (23)$$

Finally, combining Eqs. (22) and (23), we obtain $R_{21} = 0.336 \times 0.843\omega_+ = 0.283\omega_+$, and $k_{21} = 0.283k_+$.

k_{12} and k_{32} are obtained from the principle of detailed balance [Eq. (5)]. The present experiment does not provide enough information to obtain meaningful values of k_{13} and k_{31} . Table I lists the four rate coefficients for fine-structure mixing in the barium $6s5d^3D_J$ metastable levels due to collisions with argon that we have determined.

The principal sources of uncertainty in the values of the k_{ij} 's include statistical uncertainty in the fits of the buildup rates (Fig. 4) and in the least-squares fits of the slopes (Fig. 5), uncertainty in the argon pressure (~ 0.2 Torr), and errors arising from our treatment of diffusion. The major source of uncertainty in modeling and removing the effects of diffusion comes from determining the initial width of the metastable atom spatial distribution, r_0 . Since $D \propto p^{-1}$ and $R_{ij} \propto p$, the mixing becomes faster and the diffusion slower as the buffer gas pressure p increases. At small p , the buildup rate is more sensitive to the diffusion correction, and is therefore more sensitive to the value of r_0 . Our experimental uncertainty in r_0 of 25% causes an uncertainty in the fitted buildup rates of 40 and 30% for 2 and 5 Torr of buffer gas, respectively. However, at 35 and 50 Torr, the uncertainties in the measured buildup rates are down to approximately 3% due to this source. The various sources of uncertainty discussed here are reflected in the error bars of Fig. 5 and in the values of the k_{ij} 's listed in Table I.

We can also make an order of magnitude estimate of the fine-structure mixing of the metastable atoms due to collisions with other barium atoms (those in either the ground or a metastable level) from the nonzero y intercepts in Fig. 5. Using the intercept values of 4.5×10^3 and 2.0×10^4 s $^{-1}$, for 3D_1 and 3D_3 (each with an approximate uncertainty of 50%), and assuming a barium number density of 1.0×10^{13} cm $^{-3}$, we determine rate coefficients of $k_{21}^{\text{Ba}} = 1.3 \times 10^{-10}$ and $k_{23}^{\text{Ba}} = 5.8 \times 10^{-10}$ cm 3 s $^{-1}$. The uncertainty in these numbers is perhaps as large as 60 or 70% when the uncertainty in the barium density is taken into account.

TABLE I. Rate coefficients for excitation transfer among the barium $6s5d^3D_J$ levels due to collisions with argon perturbers (units of 10^{-13} cm 3 s $^{-1}$)

k_{12}	1.71 ± 0.18
k_{21}	1.39 ± 0.13
k_{23}	1.42 ± 0.13
k_{32}	1.92 ± 0.16

It should be noted in this context that the heat-pipe oven, operated with an overpressure of buffer gas as in the present experiment, is not an equilibrium environment. The barium density varies spatially along the axis and such variations may change with buffer gas pressure. This effect also contributes to the uncertainty in the barium-barium mixing rate coefficients. However, as can be seen from Fig. 5, the relative contribution to the total excitation transfer rate from barium-barium collisions is small for most perturber pressures used in this work. Thus the "correction to the correction" represented by variations in the barium density and spatial distribution with changes in the buffer gas pressure can be neglected. The same argument also applies to the nitrogen quenching experiment.

B. Quenching of the 3D_J sublevels

As stated earlier, excitation transfer between the 3D_J levels is rapid when N_2 is used as the buffer gas (see Fig. 3). Consequently, we assume that these levels are populated in their equilibrium ratios given by Eq. (13). Thus for each of the three transitions of interest ($6s5d^3D_1 \rightarrow 5d6p^1D_2^o$, $6s5d^3D_2 \rightarrow 5d6p^3F_3$, and $6s5d^3D_3 \rightarrow 5d6p^3F_4$), and each buffer gas pressure, we fit the time-dependent absorption coefficients to a function of the form

$$k_v(t) = Ae^{-\omega_- t}, \quad (24)$$

in order to determine the decay rate ω_- . For each transition, the decay rates are plotted as a function of N_2 number density in order to determine the average metastable quenching rate coefficient, $k_q(^3D_J)$ (see Fig. 6). The values of k_q obtained from a least-squares fit to $\omega_- = k_q n_p$, where n_p is the perturber (in this case molecular nitrogen) density, for each of the three 3D_J levels studied are also shown in Fig. 6. Notice that the agreement between these three values is excellent, as expected. Using the average of these values, we report our best value for the barium metastable quenching rate coefficient due to collisions with N_2 :

$$k_q(^3D_J) = (3.14 \pm 0.19) \times 10^{-11} \text{ cm}^3 \text{ s}^{-1}. \quad (25)$$

One of the main sources of uncertainty in these measurements is the uncertainty in measuring the gas pressure. Nitrogen is such an efficient quencher that we had to work at pressures in the range 0.5 to 10 Torr. Due to limitations of the vacuum/gas handling system (which was designed to work primarily in the range 2–500 Torr), there is a slight problem with calibration of the pressure gauges at very low pressures. With the heat-pipe oven cold, and the valve to the roughing pump fully open, our most accurate pressure gauge (a capacitance manometer calibrated for 0–100 Torr) reads ~ 0.2 Torr. To compensate for this systematic error in the absolute pressure determination, we subtracted 0.2 Torr from all pressure readings and included a statistical error of the same size in each point used in the least-squares fits. These are reflected in the error bars shown in Fig. 6. While the relative pressure uncertainty is largest for the lower pressure points, the total statistical uncertainty is greatest for

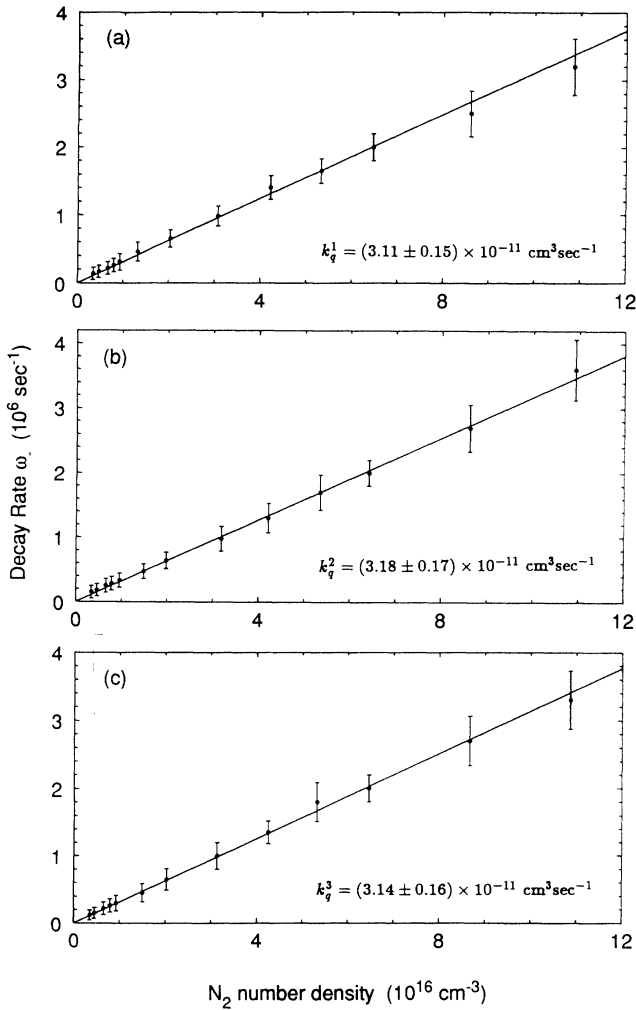


FIG. 6. Plot of the decay rate ω_- vs N_2 number density for (a) the $6s5d\ ^3D_1 \rightarrow 5d6p\ ^1D_2$, (b) the $6s5d\ ^3D_2 \rightarrow 5d6p\ ^3F_3$, and (c) the $6s5d\ ^3D_3 \rightarrow 5d6p\ ^3F_4$ transitions. The least-squares straight line fits are also shown in the figure, as well as the values of k_q determined from the slopes of the fitted lines.

the highest pressure points where the decay rates are faster, and therefore less data points are included in the fitted exponential.

Because the uncertainty in the N_2 pressure is actually systematic, there is some question as to whether it would be better to fit the data of Fig. 6 through zero, or to use an independent y -axis intercept as a second free parameter. Since the largest effect of the systematic 0.2 Torr offset was already taken into account, and any residual effect was incorporated into the error bars, we decided to fit the data through zero. However, use of a two-parameter fit (with an intercept) had little effect on the measured slope (less than 3%). This uncertainty in the fitting procedure is also included in our final value for k_q . However, one should note that if some other quenching mechanism were present, which was not a function of perturber gas density, then we would expect to see some positive y intercept in our data, and forcing the fit

through zero would be unacceptable. Quenching of the metastables by ground- or excited-state barium atoms or by ground-state Ba_2 molecules (assuming these latter exist) should, therefore, be considered.

Whitkop and Wiesenfeld [8] report a measured rate coefficient of $(1.9 \pm 0.2) \times 10^{-9} \text{ cm}^3 \text{ s}^{-1}$ for quenching of the metastable 3D_J levels by ground-state barium atoms at 730 K. If we assume that our barium density at $T = 875 \text{ K}$ is $1.0 \times 10^{13} \text{ cm}^{-3}$, we obtain a quenching rate due to ground-state barium of $\sim 2 \times 10^4 \text{ s}^{-1}$. From Fig. 6, it is evident that such a small barium quenching rate would be undetectable in the range of decay rates produced by nitrogen quenching in our experiment. Similar arguments can be made for quenching by excited barium atoms and ground-state barium molecules since the quenching rate coefficients cannot be too much larger than that reported for the ground-state atoms.

V. DISCUSSION AND CONCLUSIONS

We are aware of only one previous measurement of cross sections for excitation transfer among the $Ba(^3D_J)$ fine-structure levels due to collisions with noble gases. Kallenbach and Kock [9,10] report cross sections $\sigma_{21} = 2.7 \times 10^{-17} \text{ cm}^2$ and $\sigma_{32} = 4.0 \times 10^{-17} \text{ cm}^2$ for mixing among the 3D_J levels due to argon at $T = 1100 \text{ K}$. These values can be converted into rate coefficients (using $k_{ij} = \sigma_{ij} \bar{v}$) at $T = 857 \text{ K}$ (for comparison with the present results and assuming no temperature dependence of the cross sections) of $k_{21} = 2.1 \times 10^{-12} \text{ cm}^3 \text{ s}^{-1}$ and $k_{32} = 3.1 \times 10^{-12} \text{ cm}^3 \text{ s}^{-1}$, respectively, with a reported uncertainty of 40%. As can be seen from Table I, these values of Kallenbach and Kock are greater than those presented here by more than an order of magnitude. At present, we do not know the origin of this discrepancy. One possibility is that there is a significant temperature dependence to the mixing cross section, or that an unknown impurity could have raised the effective mixing rate in the earlier work. Also, the purpose of the work carried out by Kallenbach and Kock was to model the very complicated kinetic system produced by pumping the resonance transition $6s^2\ ^1S_0 \rightarrow 6s6p\ ^1P_1$ (using a 300-ns laser pulse with incident pulse energy of $\sim 3 \text{ mJ}$). The model involves the simultaneous fit of populations in 13 atomic levels, atomic and molecular ion densities, and electron densities and temperatures. The large uncertainties reported in that work resulted from the need to fit so many unknown (and possibly correlated) parameters simultaneously. While this must be done in order to obtain a global model of this complicated system, it is obvious that individual rate coefficients derived from the model may have substantial errors. In particular, the Kallenbach and Kock experiment was carried out at much higher barium densities than the present work, and with their high-power, long-pulse laser pumping, ionization processes were significant. Studying the ionization processes was one of the primary goals of Kallenbach and Kock. However, in the present context one must consider the possibility that electron collisions could cause an increase in the apparent mixing among the fine-structure levels in that work. The experiment we describe here was

designed specifically to measure these fine-structure mixing rates due to argon perturbers, and was relatively unencumbered by competing processes.

Kallenbach and Kock [9,10] also obtained cross sections for mixing among the 3D_J levels due to collisions with ground-state barium atoms. These values, $\sigma_{21}=3.3\times 10^{-14}$ cm² and $\sigma_{32}=5.0\times 10^{-14}$ cm², also measured at $T=1100$ K, correspond to rate coefficients at $T=857$ K of $k_{21}=1.7\times 10^{-9}$ cm³s⁻¹ and $k_{32}=2.6\times 10^{-9}$ cm³s⁻¹, respectively, with reported uncertainties of 60%. These values are also an order of magnitude greater than our present results.

Although a large body of literature exists describing theoretical calculations of cross sections for excitation transfer among atomic fine-structure levels (see Refs. [11–15] for some representative examples), all methods require knowledge of the interatomic potentials which asymptotically correlate with the individual fine-structure levels. Unfortunately, to the best of our knowledge no theoretical or experimental potentials are available which describe this Ba(3D_J)+Ar(1S_0) system, although calculated Ba($6s5d\ ^1D_2$) + rare gas and Ba($6s6p\ ^1P_1$) + rare-gas potentials are reported in Ref. [16]. Thus it is difficult to make quantitative estimates of the excitation transfer rates. However, data such as those presented here can be used to test theoretical potentials when they become available. Reference [17] presents a detailed ex-

ample of the use of measured fine-structure mixing cross sections to test various theoretical potentials in the case of K($4P_J$)+Ar. Discussions of the excitation transfer process Ba($6s6p\ ^1P_1$)+ rare gas \rightarrow Ba($6s6p\ ^3P_2$)+ rare gas in terms of potential-energy curve crossings can be found in Refs. [18–20].

To the best of our knowledge, no previous measurements of the quenching of barium 3D_J metastable atoms by nitrogen have been carried out. Eversole and Djeu [21] measured a rate coefficient of $k_q(^1D_2)=1.17\times 10^{-11}$ cm³s⁻¹ for quenching of barium $6s5d\ ^1D_2$ by molecular nitrogen. This appears to be consistent with the value reported here for the 3D_J levels. Whitkop and Wiesenfeld [8] measured a rate coefficient of $k_q^{\text{Ba}}(^3D_J)=(1.9\pm 0.2)\times 10^{-9}$ cm³s⁻¹ for quenching of 3D_J by barium perturbers. As mentioned in Sec. IV, this value is consistent with the absence of nonzero y -axis intercepts of the data of Fig. 6.

ACKNOWLEDGMENTS

The authors are grateful to Raychel Namiotka and Dr. Alan Streater for useful discussions during the course of this work. We gratefully acknowledge financial support provided by the National Science Foundation (Grant No. PHY-9119498) and the U.S. Army Research Office (Grant No. DAAH04-93-G-0063).

-
- [1] G. Magerl, B. P. Oehry, and W. Ehrlich-Schupita, ESTEC Contract No. 8488/89NL/PM(SC) Final Report (1991) (unpublished).
- [2] E. Ehrlacher and J. Huennekens, *Phys. Rev. A* **46**, 2642 (1992).
- [3] F. Beitia, F. Castaño, M. N. Sanchez Rayo, and D. Husain, *Chem. Phys.* **166**, 275 (1992).
- [4] C. R. Vidal and J. Cooper, *J. Appl. Phys.* **40**, 3370 (1969).
- [5] R. K. Namiotka, E. Ehrlacher, M. Brewer, J. Sagle, D. J. Namiotka, A. D. Streater, and J. Huennekens (unpub-Streater, and J. Huennekens (unpublished).
- [6] T. G. Walker, K. D. Bonin, and W. Happer, *J. Chem. Phys.* **87**, 660 (1987).
- [7] E. Ehrlacher, Ph.D. thesis, Lehigh University, 1993 (unpublished).
- [8] P. G. Whitkop and J. R. Wiesenfeld, *J. Chem. Phys.* **72**, 1297 (1980).
- [9] A. Kallenbach and M. Kock, *J. Phys. B* **22**, 1691 (1989).
- [10] A. Kallenbach and M. Kock, *J. Phys. B* **22**, 1705 (1989).
- [11] E. E. Nikitin, *Adv. Chem. Phys.* **28**, 317 (1975).
- [12] W. H. Miller and T. F. George, *J. Chem. Phys.* **56**, 5637 (1972).
- [13] R. H. G. Reid, *J. Phys. B* **6**, 2018 (1973).
- [14] F. Masnou-Seeuws and R. McCarroll, *J. Phys. B* **7**, 2230 (1974).
- [15] D. Lemoine, J. M. Robbe, and B. Pouilly, *J. Phys. B* **21**, 1007 (1988).
- [16] E. Czuchaj, F. Rebentrost, H. Stoll, and H. Preuss, *Chem. Phys.* **177**, 107 (1993).
- [17] J. Pascale, J.-M. Mestdagh, J. Cuvellier, and P. de Pujo, *J. Phys. B* **17**, 2627 (1984).
- [18] W. H. Breckenridge and C. N. Merrow, *J. Chem. Phys.* **88**, 2329 (1988).
- [19] J. P. Visticot, J. Berlande, J. Cuvellier, J. M. Mestdagh, P. Meynadier, P. de Pujo, O. Sublemontier, A. J. Bell, and J. G. Frey, *J. Chem Phys.* **93**, 5354 (1990).
- [20] J. P. Visticot, P. de Pujo, O. Sublemontier, A. J. Bell, J. Berlande, J. Cuvellier, T. Gustavsson, A. Lallement, J. M. Mestdagh, P. Meynadier, and A. G. Suits, *Phys. Rev. A* **45**, 6371 (1992).
- [21] J. D. Eversole and N. Djeu, *J. Chem. Phys.* **71**, 148 (1979).